New OTA-C Current-Mode Second-Order Filters

Dattaguru V. Kamath*

Abstract**—**In this paper, a general two-impedance current-mode circuit configuration with single input current using dual-output OTA is explored to derive different types of new second-order filters. The proposed biquads are attractive as they use only grounded capacitors. The proposed biquads have been realized by using various combinations of impedances like OTA based resistor, OTA based inductor and grounded capacitors in the proposed general structure. PSPICE simulation results are also given for the proposed circuits.

Keywords**—**Active filters, Biquads, Current-mode circuits, DO-OTA, OTA-C filters, SO-OTA

I. Introduction

THE OTA-C approach [1]-[13] is one of the most preferred design methods for continuous-time (CT) integrated filter design at high frequencies. The design of current-mode OTA-C filters employing active elements like Dual Output OTAs (DO-OTA) [3]-[6], [8]-[12] and Multiple Output OTAs (MO-OTA) [7], [13] have been reported. The biquads are the basic building blocks for the realization of CT filters of higher order. In the literature, different circuit configurations for realization of current-mode biquads using OTA have been described i.e., a single DO-OTA and five admittance model [5], two-integrator loop structure [2], [4], [6], [12] etc. The realization of current-mode OTA-C universal biquads using DO-OTA based general two-admittance circuit configuration [9], [10], [11], [13] has been discussed in the literature.

In this paper, the proposed DO-OTA based general current-mode two-admittance circuit structure is presented in Section II. In Section III, the proposed general basic topology is shown to be useful to realize various second-order filters by substituting various admittances in place of Y_n and Y_p. Biquads using only grounded capacitors and in some cases using floating capacitors also have been considered. The analysis of proposed biquads using single-pole finite band-width model of the OTA is considered in detail in Section IV. The summary of proposed biquads and comparison with previously reported work is presented in Section V. The SPICE simulation results are presented in Section VI to demonstrate the practical usefulness of the proposed biquads. The concluding remarks are given in Section VII.

II. Proposed DO-OTA based two-admittance circuit configuration

The circuit symbol of single output OTA (SO-OTA) and dual output OTA (DO-OTA) used in this work are shown in Fig. 1(a) and (b) respectively. The two current outputs of DO-OTA are given by

$$I_{o1}+ = I_{o2}+ = g_m(V_i^+ - V_i^-) \tag{1}$$

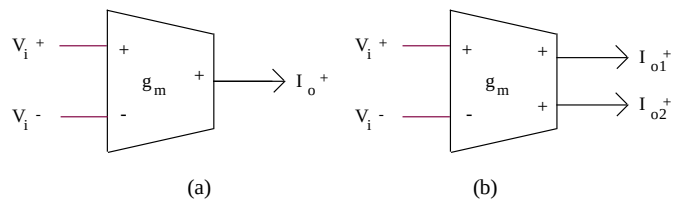

Fig. 1 Circuit symbol of (a) SO-OTA (b) DO-OTA

Here, I_{o1}^+, I_{o2}^- are the two output source currents, V_i^+ and V_i^- denote non-inverting and inverting input voltages of the DO-OTA respectively. The DO-OTA based two-admittance general current-mode configuration with two input currents has been discussed in [13]. The circuit configuration with single input current for realizing OTA-C third-order band-pass filters is shown in Fig. 2. The generalized current-input current-output (CICO) transfer function for this circuit can be shown to be

$$\frac{I_o}{I_{in}} = \frac{g_1 Y_n}{Y_p(g_1+Y_n)} \tag{2}$$

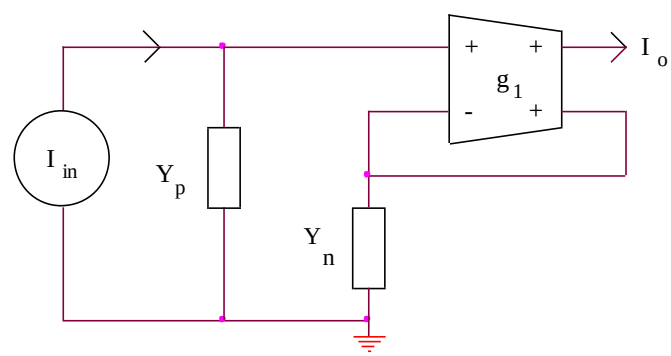

Fig. 2 DO-OTA based general current-mode two-admittance circuit configuration with single input current

III. New DO-OTA based SECOND-ORDER CURRENT-MODE OTA-C FILTERS

In this section we show that the general basic topology of Fig. 2 can be used to realize two third-order band-pass filter circuits.

A. Current-mode OTA-C second-order band-pass/ high-pass filter BP2/ HP2

The current-mode second-order band-pass/ high-pass filter circuit shown in Fig. 3 can be realized from the basic structure of Fig. 2 by replacing the admittance Y_p with grounded resistor

Dr. (Prof.) Dattaguru V. Kamath is with the Department of E&C Engg., Manipal Institute of Technology(MIT), Manipal University(MU), Manipal, India (phone: 91-09611942374 (M); e-mail: dv.kamath@manipal.edu, reachdvkamath@yahoo.com)

$1/g_2$ and Y_n with C_2 in series with grounded inductor L_1. Here the grounded inductance L_1 of value $C_1/g_3\,g_4$ is realized by OTAs g_3 and g_4 and capacitor C_2.

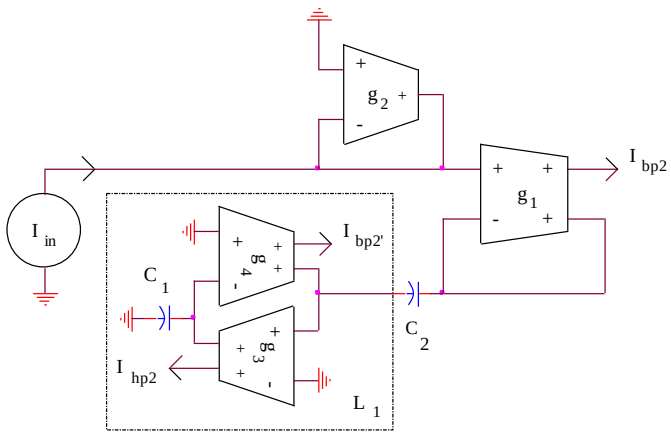

Fig. 3 Current-mode second-order band-pass/ high-pass filter BP2/ HP2 derived from the configuration of Fig. 2

The two second-order transfer functions realized by the circuit in Fig. 3 are given by

$$\frac{I_{bp2}}{I_{in}} = -\frac{I_{bp2'}}{I_{in}} = \frac{s\left(\frac{g_3 g_4}{g_2 C_1}\right)}{D(s)} \qquad (3a)$$

$$\frac{I_{hp2}}{I_{in}} = \frac{s^2\left(\frac{g_3}{g_2}\right)}{D(s)} \qquad (3b)$$

where

$$D(s) = s^2 + s\,\frac{g_3 g_4}{g_1 C_1} + \frac{g_3 g_4}{C_1 C_2}$$

The expressions for pole-frequency and pole-Q and their sensitivity values are shown to be

$$\omega_o = \sqrt{\frac{g_3 g_4}{C_1 C_2}}\,; \quad Q_o = g_1\sqrt{\frac{C_1}{g_3 g_4 C_2}} \qquad (3c)$$

$$S_{g_3}^{\omega_o} = S_{g_4}^{\omega_o} = -S_{C_1}^{\omega_o} = -S_{C_2}^{\omega_o} = 0.5$$

$$S_{C_1}^{Q_o} = -S_{g_3}^{Q_o} = -S_{g_4}^{Q_o} = -\,S_{C_2}^{Q_o} = 0.5\ ;\ S_{g_1}^{Q_o} = 1 \qquad (3d)$$

B. Current-mode OTA-C second-order low-pass/ band-pass filter LP2/ BP2

A current-mode low-pass/ band-pass biquad shown in Fig. 4 is obtained from the basic structure of Fig. 2 by replacing the admittance Y_p with grounded capacitor C_3 and Y_n with C_2 in series with grounded inductor L_1. Here the simulated grounded inductance L_1 of value $C_1/g_2\,g_3$ is realized by OTAs g_2 and g_3 and capacitor C_1.

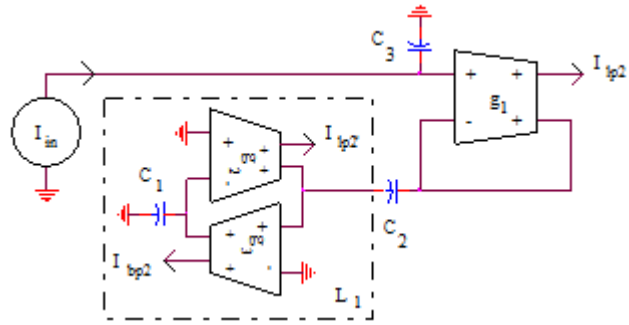

Fig. 4 Current-mode second-order low-pass/ band-pass filter LP2/ BP2 derived from the configuration of Fig. 2

The two current-mode transfer functions realized by the circuit of Fig. 4 are given by

$$\frac{I_{lp2}}{I_{in}} = -\frac{I_{lp2'}}{I_{in}} = \frac{\left(\frac{g_2 g_3}{C_1 C_3}\right)}{D(s)}$$

$$\frac{I_{lp2}}{I_{in}} = \frac{s\left(\frac{g_3}{C_3}\right)}{D(s)} \qquad (4a)$$

where

$$D(s) = s^2 + s\,\frac{g_2 g_3}{g_1 C_1} + \frac{g_2 g_3}{C_1 C_2}$$

The expressions for pole-frequency and pole-Q and their sensitivity values are shown to be

$$\omega_o = \sqrt{\frac{g_2 g_3}{C_1 C_2}}\,; \quad Q_o = g_1\sqrt{\frac{C_1}{g_2 g_3 C_2}} \qquad (4b)$$

$$S_{g_2}^{\omega_o} = S_{g_3}^{\omega_o} = -S_{C_1}^{\omega_o} = -S_{C_2}^{\omega_o} = 0.5$$

$$S_{C_1}^{Q_o} = -S_{g_2}^{Q_o} = -S_{g_3}^{Q_o} = -\,S_{C_2}^{Q_o} = 0.5\ ;\ S_{g_1}^{Q_o} = 1 \qquad (4c)$$

C. Current-mode OTA-C second-order high-pass filter HP2

A current-mode high-pass biquad shown in Fig. 5 can be realized from the basic structure of Fig. 2 by replacing the admittance Y_p with grounded inductance L_2 and Y_n with capacitor C_2 in series with grounded inductor L_1.

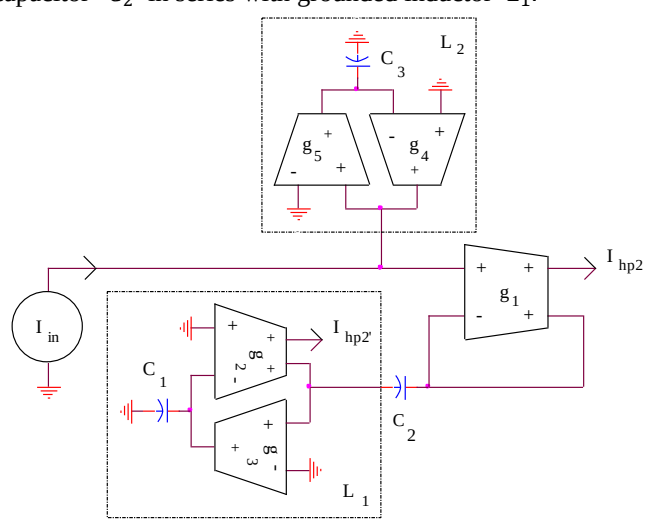

Fig. 5 Current-mode second-order high-pass filter HP2 derived from the configuration of Fig. 2

The transfer function I_{hp2}/I_{in} of the circuit of Fig. 5 is given by

$$\frac{I_{hp2}}{I_{in}} = -\frac{I_{hp2'}}{I_{in}} = \frac{\left(\frac{g_2 g_3 C_3}{g_4 g_5 C_1}\right) s^2}{s^2 + s\,\frac{g_2 g_3}{g_1 C_1} + \frac{g_2 g_3}{C_1 C_2}} \tag{5}$$

The denominator of the transfer function of this circuit is same as that for the biquad of Fig. 4. The expressions for pole-frequency and pole-Q and their sensitivity values for high-pass biquad of Fig. 5 are given by 4(b)-(c).

D. Current-mode OTA-C second-order band-stop filter BS2

The current-mode band-stop biquad shown in Fig. 6 can be realized from the basic structure of Fig. 2 by replacing the admittance Y_p with capacitor C_4 in series with grounded inductor L_2 and Y_n with C_2 in series with grounded inductor L_1.

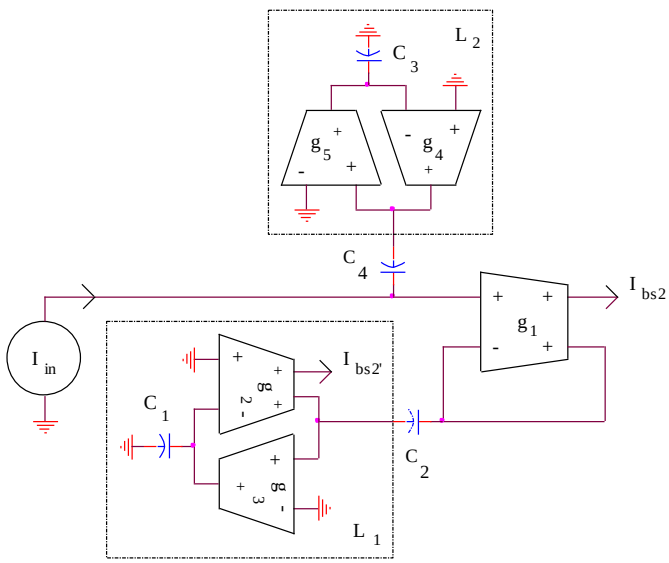

Fig. 6 Current-mode second-order band-stop filter BS2 derived from the configuration of Fig. 2

The transfer function of the circuit of Fig. 6 is given by

$$\frac{I_{o1}}{I_{in}} = \frac{\left(\frac{g_2 g_3 C_3}{g_4 g_5 C_1}\right)\left(s^2 + \frac{g_4 g_5}{C_3 C_4}\right)}{s^2 + s\,\frac{g_2 g_3}{g_1 C_1} + \frac{g_2 g_3}{C_1 C_2}} \tag{6a}$$

Under the condition $g_2 g_3 = g_4 g_5$ and $C_1 C_2 = C_3 C_4$, I_{o1}/I_{in} will implement the transfer function of a band-pass biquad given by

$$\frac{I_{bs2}}{I_{in}} = -\frac{I_{bs2'}}{I_{in}} = \frac{\left(\frac{C_3}{C_1}\right)\left(s^2 + \frac{g_2 g_3}{C_1 C_2}\right)}{s^2 + s\,\frac{g_2 g_3}{g_1 C_1} + \frac{g_2 g_3}{C_1 C_2}} \tag{6b}$$

The denominator of the transfer function of this circuit is same as that for the biquad of Fig. 4. The expressions for pole-frequency and pole-Q and their sensitivity values for high-pass biquad of Fig. 5 are given by 4(b)-(c).

E. Current-mode OTA-C second-order band-stop/ low-pass/ band-pass filter BS2/ LP2'/ BP2

A multi-function (band-stop/ low-pass/ band-pass) current-mode biquad shown in Fig. 7 can be realized from the basic structure of Fig. 2 by replacing the admittance Y_p with grounded resistor $1/g_2$ and Y_n with grounded inductor L_1 in parallel with grounded capacitor C_2. Here the inductance L_1 of value $C_1/g_3\,g_4$ is realized by OTAs g_3 and g_4 and capacitor C_1.

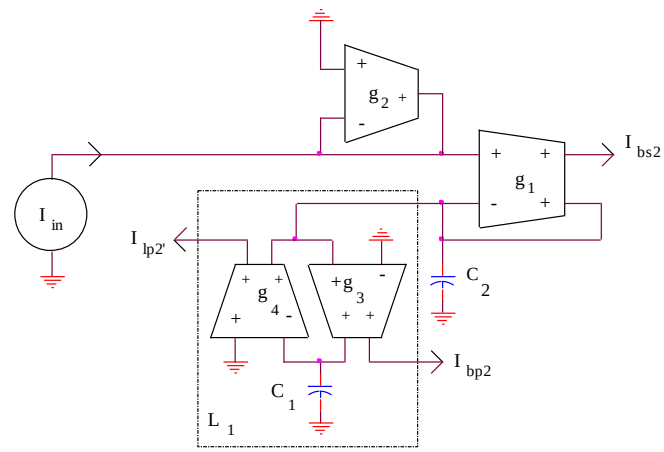

Fig. 7 Current-mode second-order multi-function (band-stop/ low-pass/ band-pass) derived from the configuration of Fig. 2

The various second-order transfer functions realized by the circuit in Fig. 7 are given by

$$\frac{I_{bs2}}{I_{in}} = \frac{\left(\frac{g_1}{g_2}\right)\left(s^2 + \frac{g_3 g_4}{C_1 C_2}\right)}{D(s)} \tag{7a}$$

$$\frac{I_{lp2'}}{I_{in}} = -\frac{\left(\frac{g_1}{g_2}\right)\left(\frac{g_3 g_4}{C_1 C_2}\right)}{D(s)} \tag{7b}$$

$$\frac{I_{bp2}}{I_{in}} = \frac{\left(\frac{g_3}{g_2}\right) s \left(\frac{g_1}{C_2}\right)}{D(s)} \tag{7c}$$

where

$$D(s) = s^2 + s\frac{g_1}{C_2} + \frac{g_3 g_4}{C_1 C_2}$$

The expressions for pole-frequency and pole-Q and their sensitivity values for multi-function biquad of Fig. 7 are shown to be

$$\omega_o = \sqrt{\frac{g_3 g_4}{C_1 C_2}}\,; \quad Q_o = \frac{1}{g_1}\sqrt{\frac{g_3 g_4 C_2}{C_1}} \tag{7d}$$

$$S_{g_3}^{\omega_o} = S_{g_4}^{\omega_o} = -S_{C_1}^{\omega_o} = -S_{C_2}^{\omega_o} = 0.5$$

$$S_{g_3}^{Q_o} = S_{g_4}^{Q_o} = S_{C_2}^{Q_o} = -S_{C_1}^{Q_o} = 0.5\ ;\ S_{g_1}^{Q_o} = -1 \tag{7e}$$

IV. Effect Of OTA Non-Idealities

In this section, we consider the effect of non-ideal frequency-dependent g_m of the OTAs on the transfer function

of the proposed biquads. The single-pole model of the OTA [4] is given by

$$g_m(s) = \frac{g_{m0}}{(1+s\tau)} \tag{8a}$$

Here, $\tau = 1/\omega_p$ where ω_p is the dominant pole frequency of the OTA.

Considering the single-pole model of the OTA given by (8a), the denominator of the transfer function (3a)-(3b) for the circuit of Fig. 3 can be shown to be

$$D(s) = s^4 g_{10}C_1C_2\tau_3\tau_4 + s^3 g_{10}C_1C_2(\tau_3+\tau_4) + s^2(g_{10}C_1C_2 + g_{30}g_{40}C_2\tau_1) + s g_{30}g_{40}C_2 + g_{30}g_{40}g_{10} \tag{8b}$$

By neglecting the s^4 term in (8b) and substituting $s^3 = -s\omega_o^2$ based on the Akerberg-Mossberg approximation [14] so as to obtain the second-order expression

$$D(s) = s^2(g_{10}C_1C_2 + g_{30}g_{40}C_2\tau_1) + s\left(g_{30}g_{40}C_2 - \omega_o^2 g_{10}C_1C_2(\tau_3+\tau_4)\right) + g_{30}g_{40}g_{10} \tag{8c}$$

Note that the pole-frequency and pole-Q are affected by the bandwidths of the OTAs:

$$\frac{\omega_p}{\omega_p{}'} = \sqrt{1 + \frac{g_{30}g_{40}\tau_1}{g_{10}C_1}} = \sqrt{1 + \left(\frac{\omega_p}{Q_p}\right)\tau_1}$$

and

$$\frac{\omega_p Q_p}{\omega_{p'} Q_{p'}} = \left(1 - \omega_p Q_p(\tau_3+\tau_4)\right) \tag{8d}$$

where the primes indicate the perturbed values of pole-frequency and pole-Q.

Note that the denominator of the transfer function is of the same type for the biquad circuits of Fig. 3, Fig. 4, Fig. 5 and Fig. 6.

Considering the single-pole finite bandwidth model of the OTA, the denominator of the transfer function (7a)-(7c) for the circuit of Fig. 7 will be of fifth-order polynomial and can be shown to be

$$D(s) = s^5\left(\frac{\tau_1\tau_3\tau_4}{\omega_p^2}\right) + s^4\frac{(\tau_1\tau_3+\tau_1\tau_4+\tau_3\tau_4)}{\omega_p^2} + s^3\left(\frac{(\tau_1+\tau_3+\tau_4)}{\omega_p^2} + \frac{\tau_3\tau_4}{\omega_p Q_p}\right) + s^2\left(\frac{(\tau_3+\tau_4)}{\omega_p Q_p} + \frac{1}{\omega_p^2}\right) + s\left(\frac{1}{\omega_p Q_p} + \tau_1\right) + 1 \tag{9a}$$

Evidently the pole-frequency and pole-Q are affected by the bandwidths of the OTAs:

$$\frac{\omega_p{}^2}{\omega_{p'}{}^2} = 1 + (\tau_3+\tau_4)\left(\frac{\omega_p}{Q_p}\right)$$

and

$$\frac{\omega_p Q_p}{\omega_{p'} Q_{p'}} = \left(1 - \omega_p Q_p(\tau_3+\tau_4) - \tau_3\tau_4\omega_p^2\right) \tag{9b}$$

V. Summary Of Proposed Biquads

In this section, the proposed current-mode biquad filter circuits are compared with the current-mode biquads available in literature. In Table 1 the proposed biquads are compared with the filters presented in [6], [8]-[12]. The proposed current-mode multi-function biquad of Fig. 7 use only grounded capacitors, whereas other biquads (of Fig. 3, Fig. 4, Fig. 5 and Fig. 6) need one or two floating capacitor(s). All The proposed biquads provide good sensitivity with respect to variations in component (transconductor and capacitance) values. The proposed biquads offer advantageous features like ease of design, programmability and orthogonal tunability of pole-Q and pole frequency.

TABLE I
Comparative Summary Of Various Current-Mode Biquads

Author /Reference	Filter types realized	No. of OTAs	No. of extra inputs/ OTA outputs	No. of capacitors (grounded/ floating)	Independent pole-Q and pole-freq. control
Fig.4(a) in Sun and Fidler [6]	LP, HP, BP, BS	6	3 inputs and 5 outputs	2 grounded	Yes
Fig.4(b) in Sun and Fidler [6]	LP, HP, BP	5	2 inputs and 4 outputs	2 grounded	Yes
Fig.4(c)&(d) in Sun and Fidler [6]	LP, BP	5	2 inputs and 3 outputs	2 grounded	Yes
Fig.5(a) in Sun and Fidler [6]	LP, HP, BP, BS	4	2 inputs and 4 outputs	2 grounded	Yes
Fig.5(b) in Sun and Fidler [6]	LP, BP	4	2 inputs and 4 outputs	2 grounded	No
Fig.5(c) in Sun and Fidler [6]	LP, BP	2	2 inputs and 2 outputs	2 grounded	No
Fig.5(d) in Sun and Fidler [6]	LP, BP	3	2 inputs and 2 outputs	2 grounded	Yes
Fig.5(e) in Sun and Fidler [6]	LP, BP	3	1 input and 2 outputs	2 grounded	Yes
Biquad#1 (Fig. 6) in Wu and El-Masry [8]	LP, BP	3	1 input and 1 output	2 grounded	No
Biquad#2 (Fig. 7) in Wu and El-Masry [8]	LP, HP, BS	4	2 inputs and 2 outputs	2 grounded	No
Biquad (Fig. 4) in Chang [9]	LP, HP, BP, BS	3	2 inputs and 3 outputs	2 grounded	No
Biquad (Fig. 5) in Chang [9]	LP, BP	2	1 input and 3 outputs	2 grounded	No
Biquad (Fig. 5) in Chang and Pai [10]	LP, HP, BP,BS, AP	2	2 inputs and 5 outputs	2 grounded	No
Biquad (Fig. 1(a)) in Bhaskar and Senani [11]	LP, HP, BP	4	6 outputs	2 grounded	No
Biquad (Fig. 1(b)) in Bhaskar and Senani [11]	LP, BP,BS	4	3 outputs	2 grounded	No
Biquad (Fig. 2) in Tsukutani [12]	LP, BP	5	3 outputs	2 grounded	Yes

Biquad (Fig. 3) in this paper	BP, HP	4	2 outputs	1 floating 1 grounded	Yes
Biquad (Fig. 4) in this paper	LP, BP	3	2 outputs	1 floating 2 grounded	Yes
Biquad (Fig. 5) in this paper	HP	5	1 output	1 floating 2 grounded	Yes
Biquad (Fig. 6) in this paper	BS	5	1 output	2 floating 2 grounded	Yes
Biquad (Fig. 7) in this paper	BS, BP, LP	4	3 outputs	2 grounded	Yes

LP: LOW PASS, HP: HIGH PASS, BP: BAND PASS, BS: BAND STOP

VI. SIMULATION RESULTS

The schematic circuit of SO-OTA and DO-OTA analog blocks used in the simulation of proposed DO-OTA based current-mode biquads are presented in Fig. 8 (a)-(b). The proposed current-mode biquads have been simulated using PSPICE simulator using the design details given in Table II. The proposed biquads were also simulated using behavioral voltage controlled current source (VCCS) model of an ideal OTA (i.e., transconductor with infinite R_o and zero C_o) to obtain the ideal characteristics.

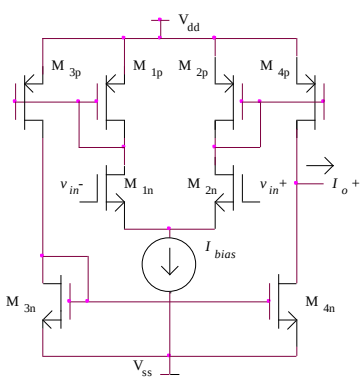

(a)

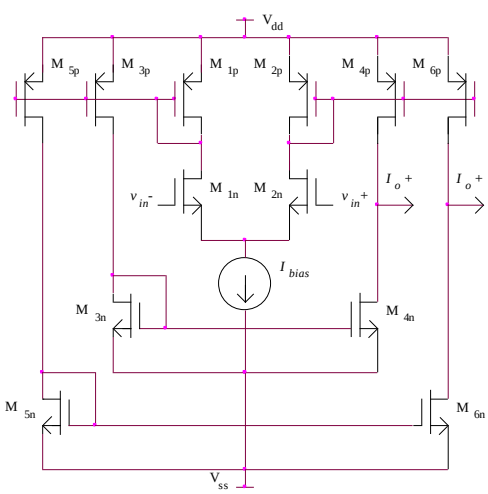

(b)

Fig. 8 CMOS schematic circuit of (a) SO-OTA (b) DO-OTA

TABLE II
SIMULATION DETAILS

Model parameters used	Level 3 0.5μm MOSIS
Device dimensions for NMOS transistor	$W = 4$ μm, $L = 2$ μm
Device dimensions for PMOS transistor	
Supply voltages	$V_{dd} = +2V, V_{ss} = -2V$

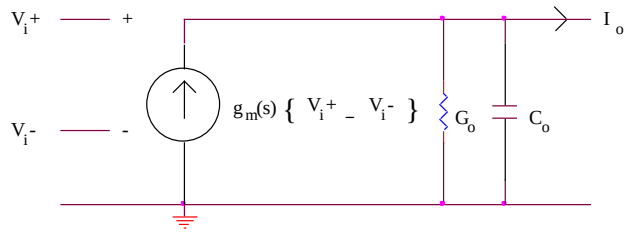

(a)

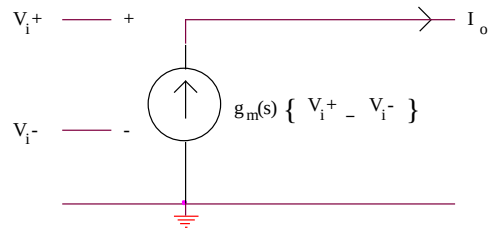

(b)

Fig. 9 (a) Non-ideal and (b) Ideal VCCS model of SO-OTA

The band-pass/ high-pass biquad filter of Fig. 3 have been simulated using $g_1 = 114$ μS ($I_{bias1} = 50$ μA), $g_2 = g_3 = g_4 = 53.9$ μS ($I_{bias2} = I_{bias3} = I_{bias4} = 10$ μA), $C_1 = C_2 = 8.58$ pF designed for a pole frequency of 1 MHz corresponding to pole-Q $Q_o = 2.12$ and the resulting amplitude responses are shown in Fig. 10.

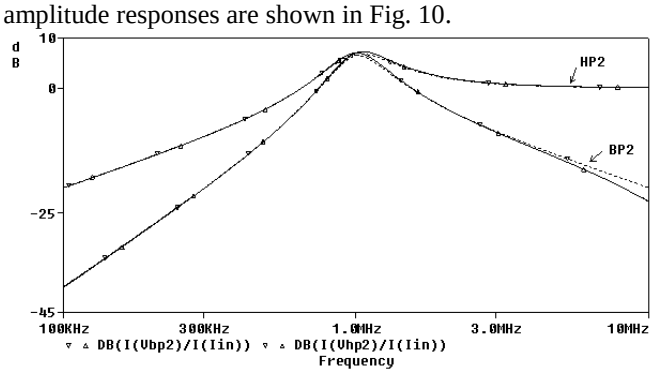

∇ …. using behavioral OTA, Δ __ using Tsukutani OTA

Fig. 10 Amplitude response of DO-OTA based BP2/ HP2 biquad of Fig. 3

The low-pass/ band-pass biquad filter of Fig. 4 has been simulated using $g_1 = 114$ μS ($I_{bias1} = 50$ μA), $g_2 = g_3 = 53.9$ μS ($I_{bias2} = I_{bias3} = 10$ μA), $C_1 = C_2 = C_3 = 8.58$ pF designed for a pole frequency of 1 MHz corresponding to pole-Q $Q_o = 2.12$ and the resulting amplitude responses are shown in Fig. 11.

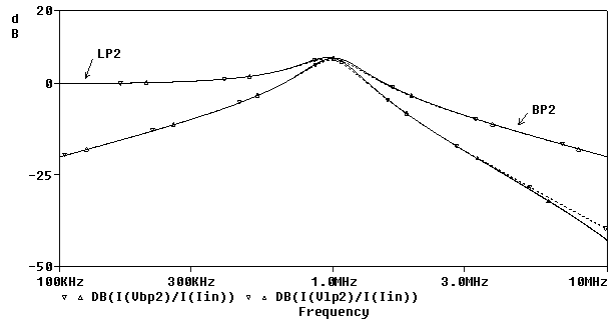

∇ …. using behavioral OTA, Δ __ using Tsukutani OTA

Fig. 11 Amplitude response of DO-OTA based LP2/ BP2 biquad of Fig. 4

The high-pass biquad filter of Fig. 5 has been simulated using $g_1 = 114\ \mu S\ (I_{bias1} = 50\ \mu A)$, $g_2 = g_3 = g_4 = g_5 = 53.9\ \mu S\ (I_{bias2} = I_{bias3} = I_{bias4} = I_{bias5} = 10\ \mu A)$, $C_1 = C_2 = C_3 = 8.58$ pF designed for a pole frequency of 1 MHz corresponding to pole-Q Q_o = 2.12 and the resulting amplitude response plot is shown in Fig. 12.

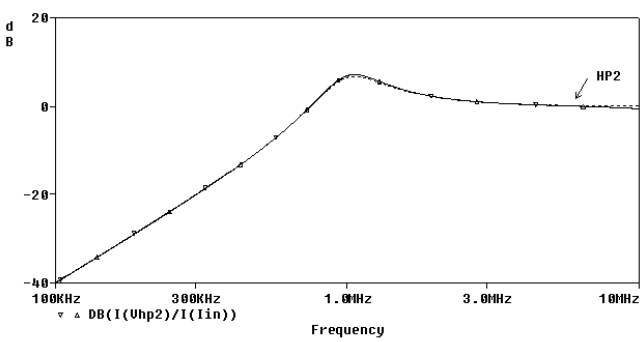

∇ …. using behavioral OTA, Δ __ using Tsukutani OTA

Fig. 12 Amplitude response of DO-OTA based HP2 biquad of Fig. 5

The band-stop biquad filter of Fig. 6 has been simulated using $g_1 = 114\ \mu S\ (I_{bias1} = 50\ \mu A)$, $g_2 = g_3 = g_4 = g_5 = 53.9\ \mu S\ (I_{bias2} = I_{bias3} = I_{bias4} = I_{bias5} = 10\ \mu A)$, $C_1 = C_2 = C_3 = C_4 = 8.58$ pF designed for a pole frequency of 1 MHz corresponding to pole-Q Q_o = 2.12 and the resulting amplitude response plot is shown in Fig. 13.

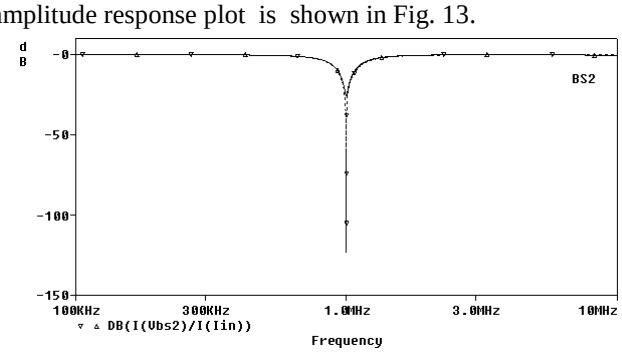

∇ …. using behavioral OTA, Δ __ using Tsukutani OTA

Fig. 13 Amplitude response of DO-OTA based HP2 biquad of Fig. 6

The band-stop/ low-pass/ band-pass biquad filter of Fig. 7 has been simulated using $g_1 = 53.9\ \mu S\ (I_{bias1} = 10\ \mu A)$, $g_2 = g_3 = g_4 = 114\ \mu S\ (I_{bias2} = I_{bias3} = I_{bias4} = 50\ \mu A)$, $C_1 = C_2 = 8.58$ pF designed for a pole frequency of 2.115 MHz corresponding to pole-Q Q_o = 2.12 and the resulting amplitude response plot is shown in Fig. 14.

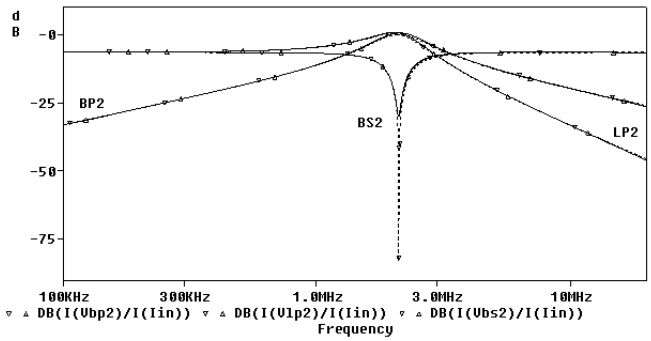

∇ …. using behavioral OTA, Δ __ using Tsukutani OTA

Fig. 14 Amplitude response of DO-OTA based BS2/ LP2/ BP2 biquad of Fig. 7

PSPICE simulations are carried out for the proposed second-order filter circuits to verify the theoretical results. The simulated results obtained using Tsukutani [12] OTA are in good agreement with the ideal plots obtained using behavioral OTA macro model.

VII. Conclusion

The proposed DO-OTA based two-admittance circuit configuration is shown to realize five different second-order filter types having advantageous features like ease of design, programmability, good sensitivity and independent pole-Q and pole-frequency control. The use of basic general topology for possible realization of third-order OTA-C filters can be investigated.

References

[1] R. L. Geiger and E. Sanchez-Sinencio, "Active filter design using operational transconductance amplifiers: a tutorial," *IEEE Circuit and Devices Magazine*, vol. 1, pp. 20-32, 1985. http://dx.doi.org/10.1109/MCD.1985.6311946

[2] R. Schaumann, M.S. Ghausi and K.R. Laker, Design of Analog Filters: Passive, Active RC, and Switched Capacitor, *Prentice Hall: Englewood Cliffs, NJ*, 1990.

[3] C. Toumazou, J. Lidgey and D. Haigh, (eds), Analogue IC Design: The Current-Mode Approach, *IEE: London, U.K*, 1990.

[4] T. Deliyannis, Y. Sun, and J. K. Fidler, Continuous-Time Active Filter Design, *CRC Press, Florida, U.S.A*, 1999.

[5] B. M. Al-Hashimi, "Current mode filter structure based on dual output transconductance amplifiers," *Electronics Letters*, vol. 32, pp. 25-26, 1996. http://dx.doi.org/10.1049/el:19960016

[6] Y. Sun, and J. K. Fidler, "Structure Generation of Current-mode Two-Integrator Loop Dual Output-OTA Grounded Capacitor Filters," *IEEE Trans. Circuits and Syst. II: Analog and Digital Signal Processing*, vol. 43, pp. 659-663, 1996. http://dx.doi.org/10.1109/82.536762

[7] Y. Sun, "Design of current-mode multiple output OTA and capacitor filters," *International Journal of Electronics*, vol. 81, no. 1, 1996. http://dx.doi.org/10.1080/002072196136959

[8] J. Wu, and E.I. El-Masry, "Design of Current-mode ladder filters using coupled biquads," *IEEE Transactions on Circuits and Systems-II: Analog and Digital Signal Processing*, vol. 45, no. 11, pp. 1445-1454, 1998.

[9] C. M. Chang, "New multifunction OTA-C biquads," *IEEE Transactions on Circuits and Systems-II: Analog and Digital Signal Processing*, vol. 46, no. 6, pp. 820-824, 1999.

[10] C. M. Chang and S.K. Pai, "Universal Current-Mode OTA-C Biquad with the Minimum Components," *IEEE Transactions on Circuits and Systems-I: Fundamental Theory and Applications*, vol. 47, no. 8, pp. 1235-1238, 2000. http://dx.doi.org/10.1109/81.873877

[11] D. R. Bhaskar, A. K. Singh, R. K. Sharma and R. Senani, New OTA-C universal current-mode/transadmittance biquads, *IEICE Electronics Express*, vol. 2, no. 1, pp. 8- 13, 2005. http://dx.doi.org/10.1587/elex.2.8

[12] T. Tsukutani, Y. Sumi, and Y. Fukui, "Electronically tunable current-mode OTA-C biquad using two-integrator loop structure," *Frequenz*, vol. 60, pp. 53-56, 2006. http://dx.doi.org/10.1515/FREQ.2006.60.3-4.53

[13] Dattaguru V. Kamath, P. V. Anandamohan and K. Gopalkrishna Prabhu, "Novel first order and second order current-mode filters using multiple output operational transconsuctance amplifiers," *Circuits, Systems, and Signal Processing, Birkhäuser Boston Publishers*, vol. 29, no. 3, pp. 553-576, 2010.

[14] D. Akerberg and K. Mossberg, A versatile Active RC building block with inherent compensation for the finite bandwidth of the amplifier, *IEEE Transactions on Circuits and Systems*, vol. 21, pp. 75-78, 1974. http://dx.doi.org/10.1109/TCS.1974.1083785

Dr. D. V. Kamath obtained PhD in the field of Analog VLSI Signal Processing from Manipal University, Manipal in the year 2013. He obtained B.E (Electronics and Communication) and M.E (Digital electronics) from B. V. Bhoomreddi College of Engineering and Technology, Karnataka University, Dharwad in the year 1987 and 1997 respectively. Currently working as Professor in the Department of Electronics and Communication Engineering, Manipal Institute of Technology, Manipal, University, Manipal, India. The research and academic contribution includes one US patent, 6 full regular papers published in indexed international journals of good repute, 4 indexed international conference publications. Author's areas of research interest include Digital, Analog and Mixed Signal VLSI design and Analog VLSI Signal Processing.

He has presented/ conducted key-note address/ tutorials and seminars at various International/ National Level Conferences/ Workshops. Author's Biography/ Profile is published in the 2011-2012 (11th) Edition of Marquis Who's Who in Science and Engineering and 2014 (31st) and 2015 (32nd) Edition of Marquis Who's Who in the World, the world-renowned reference directories. He serves as a reviewer for many international journals and he is member in international professional organizations.